

Article

Experimental and Theoretical Investigation of Supercritical Processes: Kinetics of Phase Transitions in Binary “2-Propanol—CO₂” System

Ekaterina Suslova , Maria Mochalova  and Artem Lebedev 

Department of Chemical and Pharmaceutical Engineering, D. I. Mendeleev University of Chemical Technology of Russia, 125047 Moscow, Russia; mochalovamarie@yandex.ru (M.M.); artem.evg.lebedev@gmail.com (A.L.)

* Correspondence: suslova.ekaterina.nik@mail.ru

Abstract: Studies of phase transition kinetics are important for such supercritical processes as supercritical drying, adsorption, micronization, etc. In supercritical technologies, “organic solvent—CO₂” systems are often formed, the properties of which strongly depend on the system parameters. In this article, the kinetic curves of phase transitions in the “2-propanol—CO₂” system were investigated experimentally and theoretically. Experimental studies were carried out in a 250 mL high-pressure apparatus at temperatures of 313 and 333 K and pressures of 6.3 and 7.8 MPa with and without the addition of alginate porous gel. Theoretical studies were carried out using the mass transfer equation, the Peng-Robinson equation of state, and the Van der Waals mixing rules, with Python being used for the calculations. The mass transfer coefficients and equilibrium concentrations of CO₂ in the liquid phase were determined using the BFGS optimization method.

Keywords: supercritical technology; kinetics of phase transitions; “2-propanol—CO₂” system; mass transfer coefficient



Citation: Suslova, E.; Mochalova, M.; Lebedev, A. Experimental and Theoretical Investigation of Supercritical Processes: Kinetics of Phase Transitions in Binary “2-Propanol—CO₂” System. *Computation* **2023**, *11*, 122. <https://doi.org/10.3390/computation11070122>

Academic Editor: Alexander Novikov

Received: 29 May 2023

Revised: 19 June 2023

Accepted: 19 June 2023

Published: 22 June 2023



Copyright: © 2023 by the authors. Licensee MDPI, Basel, Switzerland. This article is an open access article distributed under the terms and conditions of the Creative Commons Attribution (CC BY) license (<https://creativecommons.org/licenses/by/4.0/>).

1. Introduction

Currently, supercritical technologies are a promising emerging field that finds applications in a wide variety of industries [1–3]. Carbon dioxide is mainly used as a supercritical fluid in supercritical processes (SC-CO₂) [4,5] since it is non-toxic, non-flammable, cheap, and readily available. Moreover, it has low critical parameters ($T_c = 31\text{ °C}$, $P_c = 7.3\text{ MPa}$) [6]. If an organic solvent is used in these processes, a binary “organic solvent—CO₂” system is formed. To gain a deeper understanding of mass transfer processes under sub- and supercritical conditions, it is necessary to study the phase behavior and kinetics of phase transitions in such systems. In many cases, it is also important to consider a system in the presence of porous material. New relationships for mass transfer help to intensify the supercritical extraction process by using phase behavior and kinetics data of the binary “extracted substance—CO₂” system [7,8]. Similar data plays an important role in optimizing and scaling up different supercritical processes. In the micronization by the supercritical antisolvent (SAS) method, the “organic solvent—CO₂” system is formed. The phase behavior of this system affects the atomization process and, consequently, the final properties of the resulting material [9,10]. Additionally, data about the kinetics of phase transitions and phase behavior are important in the supercritical drying process, which is the main stage in the production of highly porous materials such as aerogels [11,12]. To produce aerogels, the organic solvent is removed from the gel by supercritical drying without its structure collapsing or shrinking. This is possible due to the supercritical state of the “organic solvent—CO₂” system formed during the process. This system is homogeneous at process parameters; thus, no phase boundary occurs inside the gel, and there are no capillary forces in the gel’s porous structure. The specified condition determines the choice of an acceptable organic solvent. The most commonly used solvents are methanol,

ethanol, 2-propanol, acetone, hexane, etc. [13–16]. The supercritical drying process can be divided into four stages: during pressurization, there is a pressure increase and the phase transitions of the binary “organic solvent—CO₂” system. The next steps are the displacement of the organic solvent from the free volume of the apparatus and the further diffusional exchange of the organic solvent inside the gel with SC-CO₂. The final step is isothermal depressurization.

The pressurization step is an important part of the supercritical drying process, since as the pressure in the system increases, the volume of the liquid phase increases due to the dissolution of CO₂ in an organic solvent; otherwise, spillage may occur. This phenomenon affects the transport of organic solvent from the pores of the gels, as a significant part of the solvent leaves during this step. A detailed investigation of the pressurization step of the supercritical drying process was introduced in [17]. The article shows the influence of the parameters and properties of the gel on the kinetics of spillage. These data confirm the importance of studying the kinetics of phase transitions for supercritical processes. The behavior of the “organic solvent—CO₂” system at subcritical conditions depends on the solubility of CO₂ in the organic solvent. For example, as the temperature rises to the critical point, the solubility in organic polar solvents decreases in accordance with Le Chatelier’s principle [18,19]. Thus, the dissolution process is exothermic [20]. However, with increasing pressure, the solubility of CO₂ in the liquid phase increases [21]. When the pressure is increased to critical parameters of the system, the distinction between liquid and gas phases disappears, and CO₂ becomes indefinitely mixed with the solvent.

Different binary systems of “organic solvent—CO₂” have similar phase behavior. For example, articles [22–26] provide data on phase equilibrium at various parameters of the binary system “2-propanol—CO₂,” which is often used in supercritical processes [17,27]. As the pressure in the system increases, the composition of the gas phase almost does not change, in contrast to the composition of the liquid phase. This is due to the increase in solubility of CO₂ in 2-propanol with pressure. There is a noticeable increase in liquid phase volume with pressure and corresponding mole fraction of CO₂ increasing [17]. Figure 1 demonstrates such an increase for the “2-propanol—CO₂” system as a function of pressure. The curves were calculated using phase equilibrium data and the Peng-Robinson equation of state (PR-EoS) with Van der Waals mixture rules [28].

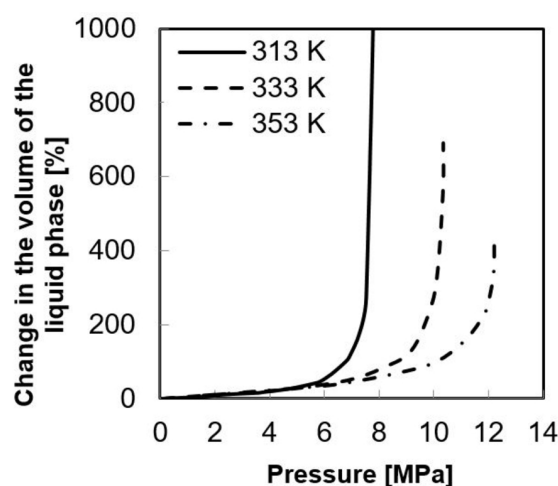


Figure 1. Liquid phase volume of the “2-propanol—CO₂” system with increasing pressure.

From the presented data (Figure 1), it can be seen that the curves asymptotically approach the critical pressures of the mixture at different temperatures. At these points, the difference between the two phases disappears, and the system becomes homogeneous.

These data are determined by the thermodynamic state of the system and do not contain any information about the rate of the processes—about the kinetics of phase

transitions. However, it is important to note that the kinetic parameters determine the course of many supercritical processes and can be used for their optimization.

When a porous body, such as a gel, is added to the binary system, the phase behavior and phase transition kinetics of the “2-propanol—CO₂” system differ from the system without a gel. The gel has small-diameter pores in which diffusion is hindered since the pore diameter is commensurate with the mean free path of a molecule. Evaluation of the effect of a porous body on the rate of phase transitions is relevant for the supercritical drying process [29,30], for solvent exchange at high pressure [31], etc.

For the study of the kinetics of phase transitions and mass transfer in binary systems, various equations of state are used, such as PR-EoS [28,32], Soave-Redlich-Kwong EoS (SRK-EoS) [33–35], Valderrama-Patel-Teja (VPT-EoS) [36,37], and mixing rules for multicomponent systems—Van der Waals’ [28,38,39], Huron-Vidal’s [40,41], and Sandler-Wong’s [42,43]. Often, the Peng-Robinson equation with Van der Waals mixing rules is used to study systems in the sub- and supercritical state since this equation is not very complex and allows for calculations with sufficient accuracy.

In this paper, the kinetics of phase transitions of the “2-propanol—CO₂” system in the presence of a model porous material—alginate gel—and without it at various process parameters were studied. A series of experiments were carried out at temperatures of 313 and 333 K and pressures of 6.30 and 7.80 MPa. The effect of an isobaric increase of temperature and an isothermal increase of pressure on the system was studied. Mass transfer coefficients were calculated using an approach based on the mass transfer equation in combination with the PR-EoS. The obtained results are necessary for the development of supercritical processes, such as supercritical drying [44], solvent exchange under pressure [31], and supercritical adsorption [45].

2. Materials and Methods

2.1. Chemicals

The following chemicals were used: Alginic acid sodium salt (AlgNa, Algin, Alginic acid sodium salt from brown algae) (CAS 9005-38-3), Sigma-Aldrich, Saint Louis, MO, USA; CaCl₂·2H₂O (CAS 10035-04-8), purity ≥ 99.5%, Sigma-Aldrich; 2-propanol, purity ≥ 99.5%, RusHim, Moscow, Russia; CO₂, purity ≥ 99.8%, ITC-Pex, Moscow, Russia; deionized water (H₂O), prepared by laboratory water treatment equipment (Arium 61215, Sartorius) Göttingen, Germany. All chemicals were used directly without further purification.

2.2. Preparation of Alginate Gels

In this work, it was decided to use an alginate-based gel as a porous material, which is formed during the production of organic aerogels [46,47]. The production of the gel is carried out by using the dripping method in accordance with [44]. To prepare a 1 wt% solution of AlgNa in water, the required amount of AlgNa powder is poured into water and mixed on a magnetic stirrer. The resulting mixture is continuously stirred for 24 h to completely dissolve the AlgNa. Spherical particles are formed by dripping the 1 wt% solution of AlgNa drop-by-drop through a needle into the crosslinking agent (5 wt% solution of CaCl₂) with constant stirring. The resulting gel particles are kept in a CaCl₂ solution for 24 h, so that the chemical reactions proceed in full.

To study the kinetics of phase transitions, it is necessary to carry out solvent exchange in the gels with 2-propanol. To do this, the gel samples are transferred from the crosslinking agent solution to a 10 wt% 2-propanol solution, then to 30 wt%, 50 wt%, 70 wt%, and 90 wt% and twice to 100 wt% solutions. The gels are kept in each solution for 2–3 h with stirring. The exchange process takes a total of 14–21 h.

2.3. Experimental Study of the Kinetics of Phase Transitions

The study of the kinetics of phase transitions was performed using an experimental setup for supercritical processes [48]. The schematic diagram of the setup is shown in Figure 2. In order to organize the supply of 2-propanol to the apparatus setup, it was

upgraded [31]. An additional alcohol supply line was added to the setup, which consists of a dosing container 9, a membrane dosing pump 10 (Lewa, LDB1, Leonberg, Germany), a pipeline, and a shut-off valve. This line is connected to one of the upper pipes of the apparatus. The setup also has a Coriolis flow meter (Bronkhorst, mini Cori-flow M13, Ruurlo, The Netherlands) on the carbon dioxide supply line, which monitors the mass flow of the gas and determines its total mass. In addition, a video recording system is added to the setup to record the behavior of the system during phase transitions in the device with sight glasses 5.

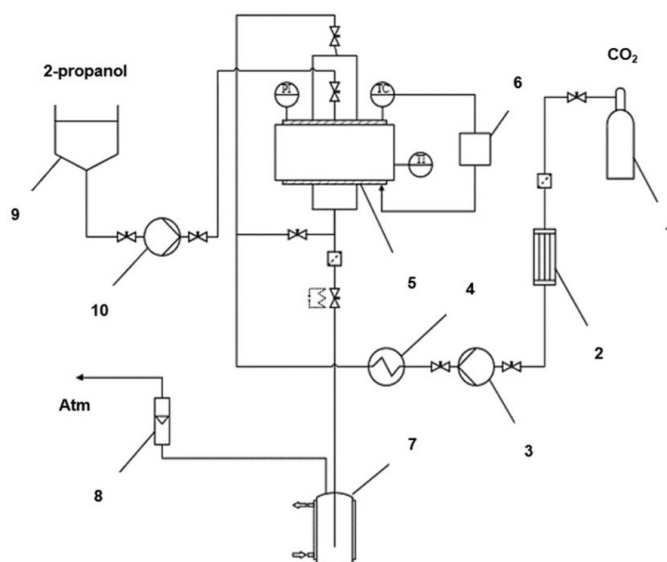


Figure 2. Schematic diagram of the equipment for conducting supercritical processes (PI—pressure probe, TC—temperature probe, TI—temperature probe).

The experimental study of the kinetics of phase transitions involves measuring the change in liquid phase volume when establishing equilibrium in the “2-propanol—CO₂” system. A 250 mL high-pressure apparatus (5) is heated to a specific temperature using the temperature control system (6). If the kinetics are being studied in the presence of a porous body, alginate gel is loaded into the apparatus and then sealed. Next, a predetermined amount of 2-propanol is fed into the apparatus from container 9 using a diaphragm pump 10 at a flow rate of 50–100 mL/min. The apparatus is then thermostated for 20 min before starting the video recording system to detect the position of the phase boundary in the apparatus. The apparatus is then fed with CO₂ from tank 1 with a flow rate of no more than 1000 g/h through condenser 2 and heating element 4, after which pressurization time does not exceed 2 min. The carbon dioxide flow rate is regulated using a metering valve, while the mass flow rate and total mass of CO₂ are determined by the Coriolis mass flowmeter and control system, respectively. The video recording of the system continues for 30–90 min before draining the 2-propanol from the apparatus through separator 7 to collect the liquid phase. Finally, the gas phase flow rate is measured using rotameter 8.

This study investigates the “2-propanol—CO₂” system under different conditions, including 313 K at 6.3 MPa and 7.8 MPa and 333 K at 6.3 MPa and 7.8 MPa.

The experiments are conducted in two stages, with repeated experiments at specified process parameters for each stage except for the “2-propanol—CO₂” system in the presence of gel at parameters 333 K and 7.8 MPa.

2.4. Image Analysis

The process of the “2-propanol—CO₂” system phase transitions was studied using a video recording system. The resulting video was converted into photographic images of the system with an interval of 2 s, which were used to determine the volume of the liquid phase at a certain point of time to obtain the kinetics curves of the phase transitions of the

system. For this purpose, the height of the liquid phase h and the diameter of the apparatus d were determined for each image (Figure 3). The height of the liquid phase volume in the images and the errors of its measurements were received using the method presented in Appendix A. The error in determination of the height of the liquid phase volume for all repeated experiments does not exceed 5%.

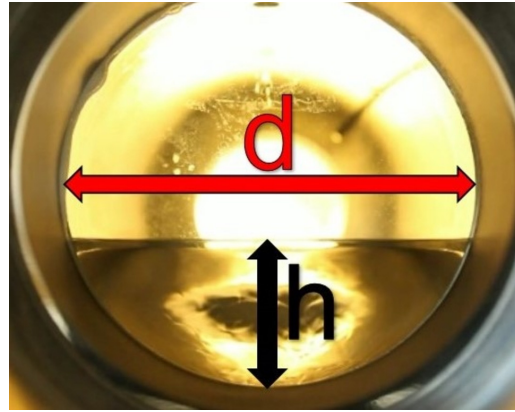


Figure 3. Processed image of the system for determining the volume of the liquid phase in the apparatus.

To determine the actual height of the liquid phase H , we took into account the ratio of the scale of the apparatus in the image and in the real setup (the diameter of the apparatus in the image d and the real diameter of the apparatus D):

$$H = \frac{D \cdot h}{d} \quad (1)$$

By using Equation (1) to calculate the real height of the liquid phase level, we can determine the volume of the liquid phase V at a certain point in time:

$$V = \left[\left(H - \frac{D}{2} \right) \cdot \sqrt{H \cdot D - H^2} + \frac{D^2}{4} \cdot \left(\frac{\pi}{2} + \arctg \left(\frac{H - \frac{D}{2}}{\sqrt{H \cdot D - H^2}} \right) \right) \right] \cdot L \quad (2)$$

Next, the change of the liquid phase volume in relation to the liquid phase initial volume $\Delta V/V_0$ is calculated:

$$\frac{\Delta V}{V_0} = \frac{V - V_0}{V_0} \cdot 100\% \quad (3)$$

Based on the obtained data on the dependence of the liquid phase volume change in time, we construct kinetics curves of the “2-propanol—CO₂” system phase transitions under various conditions.

2.5. Estimation of Mass Transfer Coefficients

To determine the mass transfer coefficients across the phase interface, a mathematical description of the kinetics of the phase transitions is proposed. To do this, the change in the liquid phase volume due to mass transfer across the interface is calculated. At the initial time, the liquid phase is pure 2-propanol, and the gas phase is pure CO₂. At the same time, it is assumed that the system is in isobaric and isothermal conditions. The total mass transfer through the phase boundary is calculated using the mass transfer equation:

$$dM = K \cdot (x^* - x) \cdot dF \cdot d\tau \quad (4)$$

where dM —the mass transfer rate, kg; K —the mass transfer coefficient, kg/(m²·s); $(x^* - x)$ —the driving force of the process; dF —the effective mass transfer area, m²; and $d\tau$ —the time step, s.

The gas and liquid phase densities are calculated using the PR-EOS with Van der Waals mixing rules [28] for multicomponent systems. The equation can be represented as a polynomial for further solution:

$$Z^3 - (1 - B) \cdot Z^2 + (A - 2B - 3B^2) \cdot Z - (AB - B^2 - B^3) = 0 \tag{5}$$

where

$$A = \frac{a \cdot P}{R^2 \cdot T^2}; B = \frac{b \cdot P}{R \cdot T}; Z = \frac{V_{mol} \cdot P}{R \cdot T} \tag{6}$$

$$a = 0.4572 \cdot \frac{(R \cdot T_c)^2}{P_c} \cdot \left[1 + m \cdot \left(1 - \sqrt{\frac{T}{T_c}} \right) \right]^2; b = 0.0778 \cdot \frac{R \cdot T_c}{P_c} \tag{7}$$

$$m = 0.3746 + 1.54226 \cdot \omega - 0.2699 \cdot \omega^2 \tag{8}$$

where P —pressure, MPa; R —gas constant, J/(mol·K); T —temperature, K; V_{mol} —molar volume, m³/mol; T_c —critical temperature, K; P_c —critical pressure, MPa; and ω —acentric factor.

The problem is then simplified by solving the cubic equation using Vieta’s trigonometric formula [49] to find the Z -coefficient of compressibility.

The equation is used to calculate the phase boundary F , through which mass transfer takes place:

$$F = L \cdot C \tag{9}$$

where L —the length of the phase boundary, m; C —the width of the phase boundary, m.

Figure 4 shows a schematic representation of the length of the phase boundary, equal to the length of the apparatus, the width of the phase boundary, and the phase boundary surface.

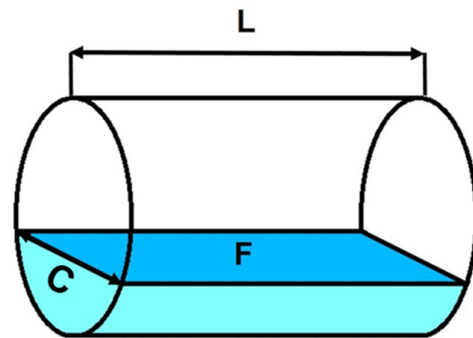


Figure 4. Schematic representation of the system in the apparatus.

The width of the boundary C is the chord of the circle of the apparatus, which is determined by geometric calculations in terms of the radius of the apparatus R and the height of the liquid level in the apparatus h :

$$C = \sqrt{4 \cdot (R^2 - (R - h)^2)} \tag{10}$$

The height of the phase boundary is calculated based on the recalculation of the volumes of the liquid and gaseous phases. The process continues until the equilibrium mole fraction is established in both the liquid and gas phases. The calculated change of the liquid phase volume is determined by Equation (3) using the calculated volume of the liquid phase at a certain point of time.

The mass transfer coefficient and equilibrium mole fraction of CO₂ in the liquid phase (2-propanol) are determined by minimizing the error between the calculated and

experimental phase transition kinetics curves. The error is calculated using the following equations:

$$Error (i) = \frac{\left| \left[\frac{\Delta V}{V_0} \right]_{calc} - \left[\frac{\Delta V}{V_0} \right]_{exp} \right|}{\left[\frac{\Delta V}{V_0} \right]_{exp}} \cdot 100\% \quad (11)$$

$$Error = \frac{\sum Error (i)}{N} \quad (12)$$

where $Error (i)$ —error of the calculated data at a certain point of time, $Error$ —average error of the calculated data for all experimental points, and N —the number of experimental points.

The minimization procedure was performed using the Broyden–Fletcher–Goldfarb–Shanno algorithm (BFGS). The algorithm was realized using the Python programming language and the SciPy library. A flowchart of the algorithm for determining the mass transfer coefficient and equilibrium mole fraction of CO₂ in the liquid phase is presented in Section 3.2. Calculated curves of the phase transition kinetics.

3. Results and Discussion

3.1. Experimental Curves of Phase Transition Kinetics

Phase transition kinetics were studied at various external parameters: pressure 6.30 and 7.80 MPa and temperature 313 and 333 K. The specified parameters were selected to study the system in a heterogeneous region. It is important to note that it is complicated to reach target parameters, but they can be easily measured with high accuracy. Therefore, the values of the measured parameters for each experiment will be presented below. During the study of the “2-propanol—CO₂” system, 50 mL of 2-propanol was preloaded into the apparatus. When studying the “2-propanol—CO₂” system in the presence of gel, 80 mL of 2-propanol and 40 mL of gel were preloaded into the apparatus. The average particle diameter of the gel that is loaded into the apparatus was 2.7 mm with a standard deviation of 0.14.

After the research, the gels were dried using supercritical drying. The porosity of the obtained aerogels was 95%, the specific surface area was 442 m²/g, the average pore diameter was 22 nm, and the pore volume was 2.19 cm³/g.

Using the approach presented above, a set of phase transition kinetics curves was obtained. Table 1 shows the parameters of the two-component “2-propanol—CO₂” system phase transition kinetics.

Table 1. Parameters of the two-component “2-propanol—CO₂” system kinetics of the phase transitions without gel addition.

Experiment	External Target Parameters		Measured External Parameters	
	Temperature, [K]	Pressure, [MPa]	Temperature, [K]	Pressure, [MPa]
1-1	313	6.30	313.83	6.13
1-2			312.99	6.34
1-3			314.35	6.48
2-1	313	7.80	312.66	7.76
2-2			312.68	7.98
2-3			314.98	7.98
3-1	333	6.30	332.95	6.50
3-2			333.38	6.34
3-3			325.28	6.67
4-1	333	7.80	333.05	7.66
4-2			333.83	7.96
4-3			333.25	7.64

Table 2 shows the parameters of the two-component “2-propanol—CO₂” system phase transition kinetics in the presence of alginate gel.

Table 2. Parameters of the two-component “2-propanol—CO₂” system kinetics of the phase transitions in the presence of the gel.

Experiment	External Target Parameters		Measured External Parameters	
	Temperature, [K]	Pressure, [MPa]	Temperature, [K]	Pressure, [MPa]
1-1	313	6.30	313.93	6.36
1-2			314.03	6.29
1-3			312.80	6.29
2-1	313	7.80	314.48	7.75
2-2			313.19	7.86
2-3			314.01	7.78
3-1	333	6.30	333.34	6.32
3-2			333.79	6.28
3-3			333.52	6.28
4-1	333	7.80	333.72	7.80
4-3			332.26	7.79

Experiment 4-2 was unsuccessful; therefore, we have excluded the data related to it from the article.

Furthermore, Figure 5 shows the apparatus at various points of time, in which the “2-propanol—CO₂” system liquid phase volume changes in the absence of alginate gel at a temperature of 312.68 K and a pressure of 7.98 MPa (Table 1, experiment 2-2). Figure 6 shows a binary system in the presence of the gel at a temperature of 313.19 K and a pressure of 7.86 MPa (Table 2, experiment 2-2).



Figure 5. Kinetics of the change in the “2-propanol—CO₂” system liquid phase volume without the addition of the alginate gel at a temperature of 312.68 K and a pressure of 7.98 MPa.

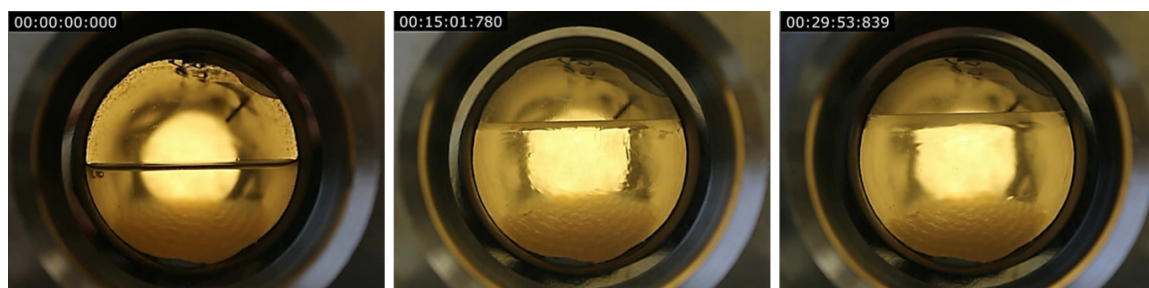


Figure 6. Kinetics of the change in the “2-propanol—CO₂” system liquid phase volume without the addition of the alginate gel at a temperature of 313.19 K and a pressure of 7.86 MPa.

To obtain the phase transitions kinetics curves, at least 40 photographic images of the “2-propanol—CO₂” system liquid phase were obtained in the apparatus at various points

of time. As a result of the processing of photographic images (see Section 2.4), the change of the liquid phase volume was determined, and the kinetic curves of the “2-propanol—CO₂” system phase transitions were obtained without and with the presence of the alginate gel (Figures 7 and 8).

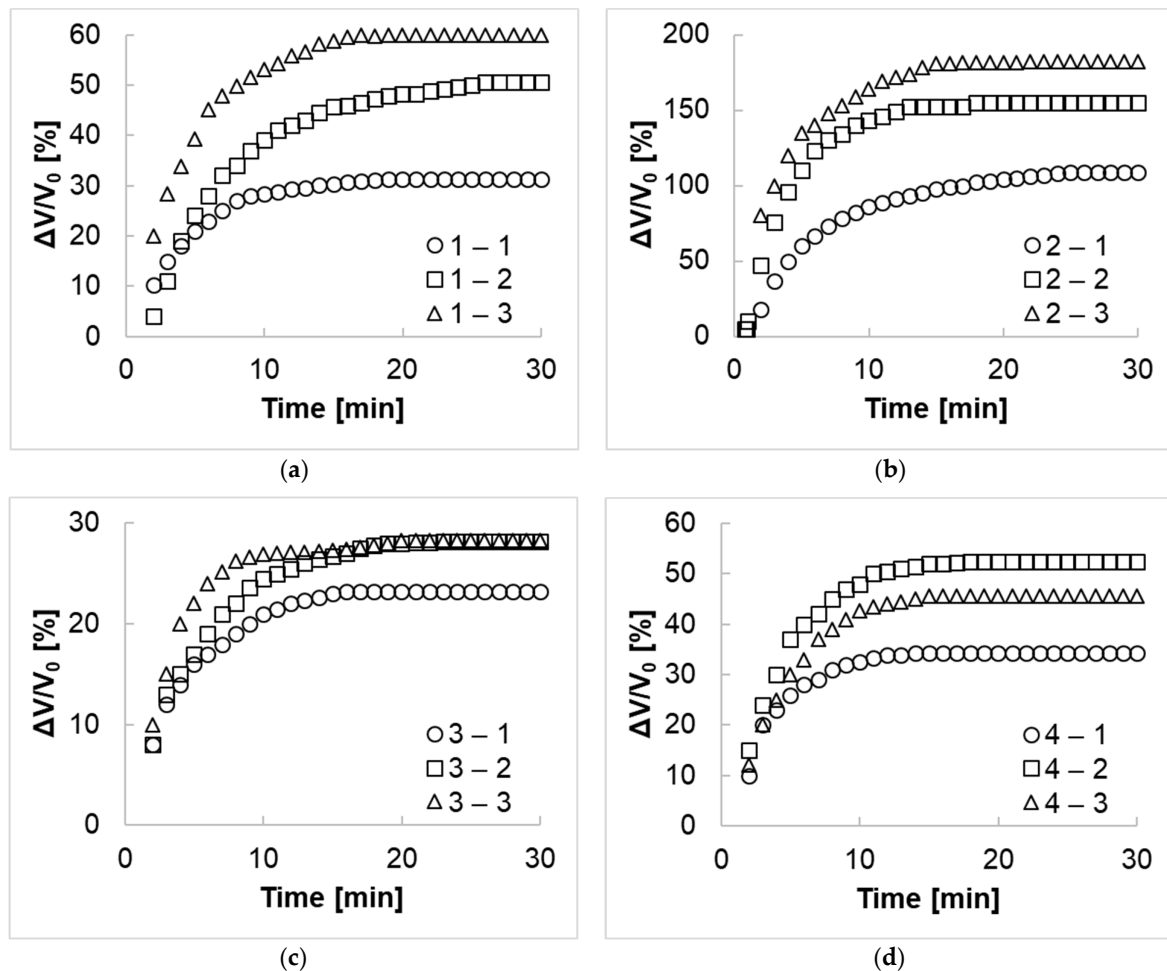


Figure 7. Phase transitions kinetics curves of a two-component “2-propanol—CO₂” system with target parameters: (a) 313 K, 6.30 MPa; (b) 313 K, 7.80 MPa; (c) 333 K, 6.30 MPa, (d) 333 K, 7.80 MPa.

The kinetic curves of the phase transitions show that the change in the process parameters (temperature and pressure) significantly affects the change of the liquid phase volume (Figure 7). With an isobaric increase in temperature, the solubility of CO₂ in the solvent decreases, which is confirmed by experimental studies. With an isothermal increase in pressure, the solubility of CO₂ increases. It is also important to note that the values of the maximum change of the liquid phase volume (when the liquid phase volume stops changing and reaches a constant level) are not the same in different experiments with the same target parameters. The measured temperature and pressure of the experiments are different from each other due to the complexity of reaching the process parameters. The maximum volume is observed at approximately 7.80 MPa and a temperature of 313 K (Figures 7 and 8b), since these parameters are close to the critical temperature and pressure of the binary mixture.

The “2-propanol—CO₂” system without gel reaches the equilibrium state in less than 30 min after the start of the process (Figure 7), in contrast to the system in the presence of the alginate gel (Figure 8). This is due to the fact that the gel is a porous material; therefore, mass transfer slows down because of the diffusion inside pores.

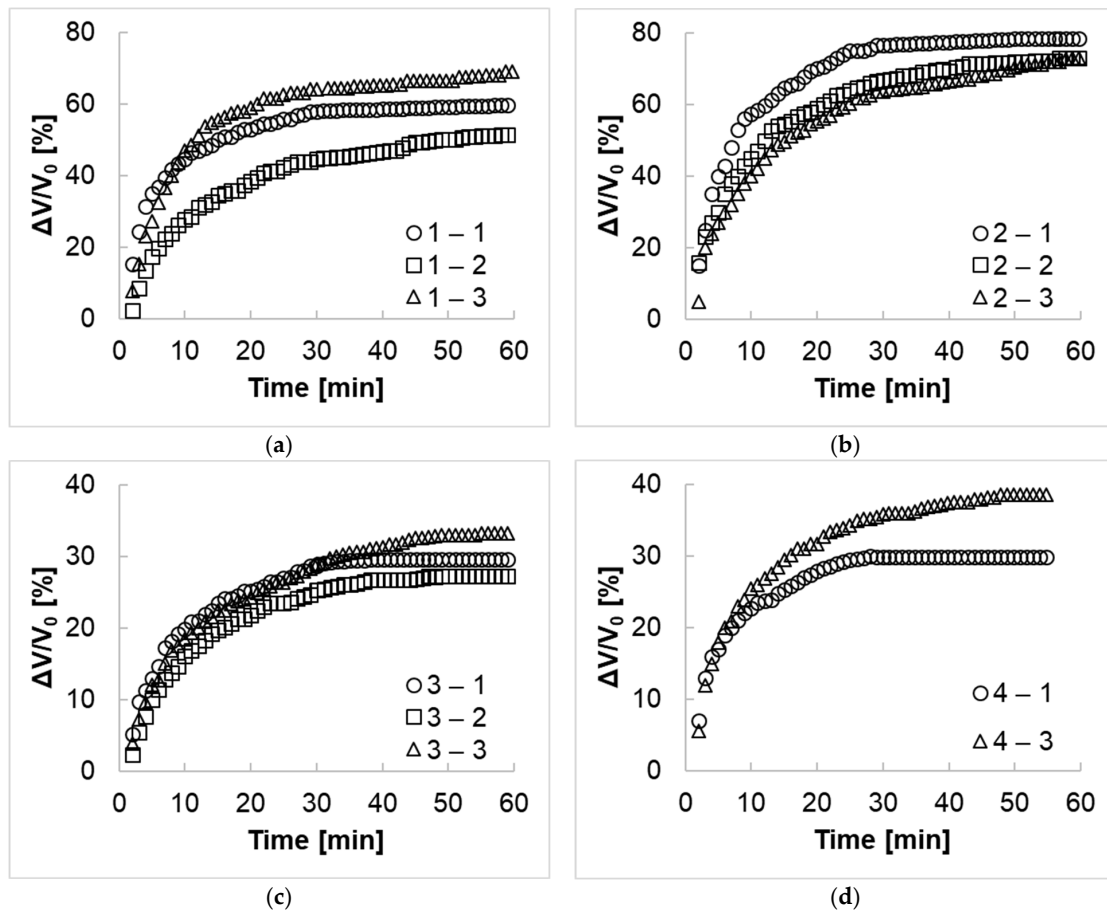


Figure 8. Phase transitions kinetics curves of the two-component “2-propanol—CO₂” system in the presence of the alginate gel at the target parameters: (a) 313 K, 6.30 MPa; (b) 313 K, 7.80 MPa; (c) 333 K, 6.30 MPa, (d) 333 K, 7.80 MPa.

3.2. Calculated Curves of the Phase Transition Kinetics

To study the effect of a porous body on the kinetics of the “2-propanol—CO₂” system phase transitions, the mass transfer coefficients of the binary system and the equilibrium mole fraction of CO₂ in the liquid phase (Section 2.5) were determined for various process parameters.

To implement this algorithm for calculating the mass transfer coefficient and the equilibrium mole fraction of CO₂ in the liquid phase, the following data must be entered:

- dV_{exp} —a list consisting of all experimental data about changes in the liquid phase volume (see Section 2.4);
- t_{exp} —a list consisting of the times at which the experimental data of the liquid phase volume change were determined;
- $T_{cr,i/j}, P_{cr,i/j}$ —critical temperature and pressure of substances, i —CO₂, j —2-propanol;
- T, P —experimental process temperature and pressure;
- D, L —geometric dimensions of the apparatus, diameter and length, respectively;
- V_0 —the liquid phase volume at the initial time is equal to the volume of pure 2-propanol;
- x —the mole fraction of CO₂, at the initial time is zero;
- F —phase contact surface area;
- $m_{i/j}$ —mass of the substance, i —CO₂, j —2-propanol (const);
- t —process time;
- dt —time step; and

- t_{end} —the time of the end of the process, which is equal to the time of the experimental study of the kinetics of phase transitions.

The mass transfer coefficient K and the equilibrium mole fraction of CO_2 in the liquid phase x^* are variables and are determined using the BFGS algorithm by finding the minimum average error between the experimental and calculated data.

A flowchart for determining the mass transfer coefficient and the equilibrium mole fraction of CO_2 in the liquid phase is shown in Figure 9.

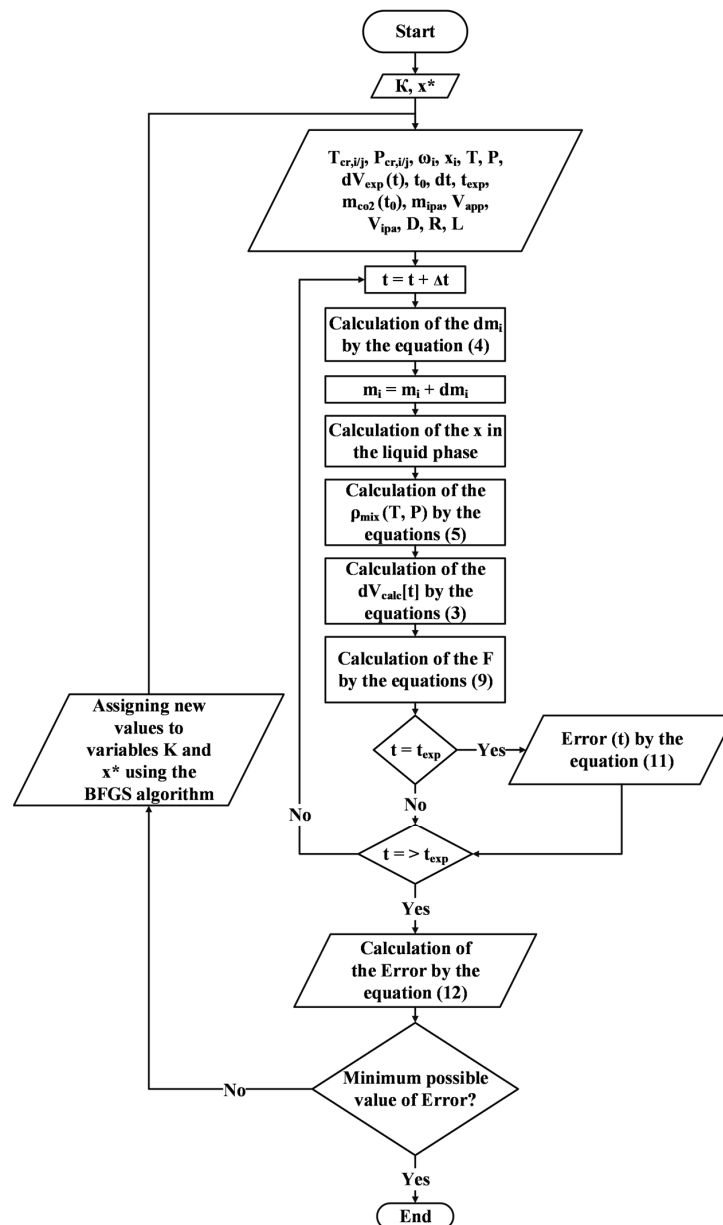


Figure 9. Flowchart for determining the mass transfer coefficient K and the equilibrium mole fraction of CO_2 in the liquid phase x .

Experimental and theoretical kinetic curves of the phase transitions of the system at different temperatures and pressures are shown in Figures 10–17.

Table 3 shows the numerical values of the calculated data obtained for all the experimentally obtained process parameters, the equilibrium mole fraction from other researches (an interpolation procedure was used for data processing in some cases), and the average error of the calculated data of kinetic curves according to experimental ones.

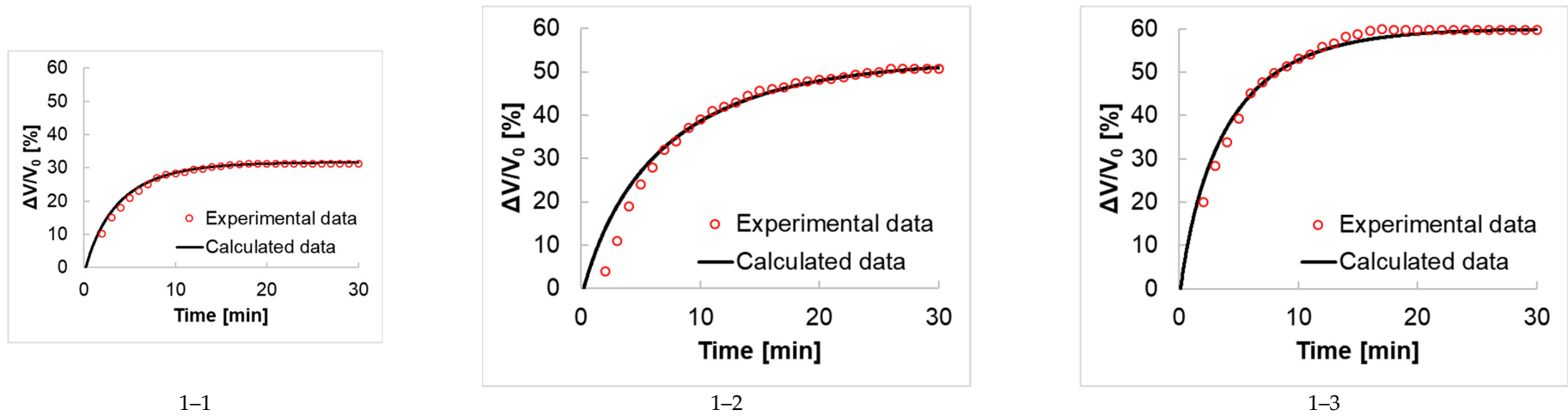


Figure 10. Experimental and calculated data of the kinetics of phase transitions at target parameters of 313 K, 6.30 MPa: experiments conducted without an alginate gel (see Table 1).

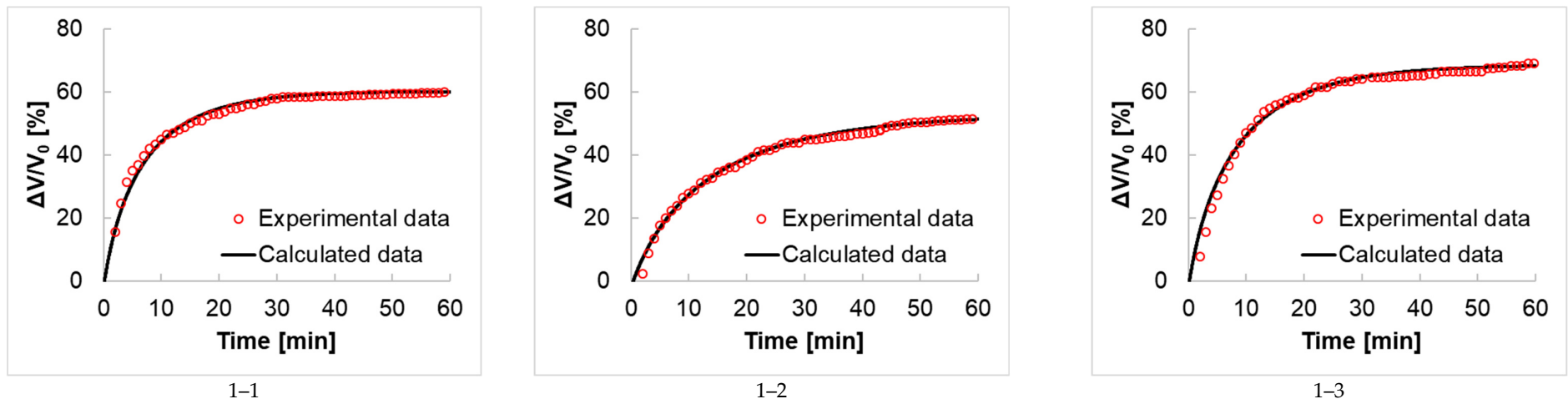


Figure 11. Experimental and calculated data of the kinetics of phase transitions at target parameters of 313 K, 6.30 MPa: experiments conducted with an alginate gel (see Table 2).

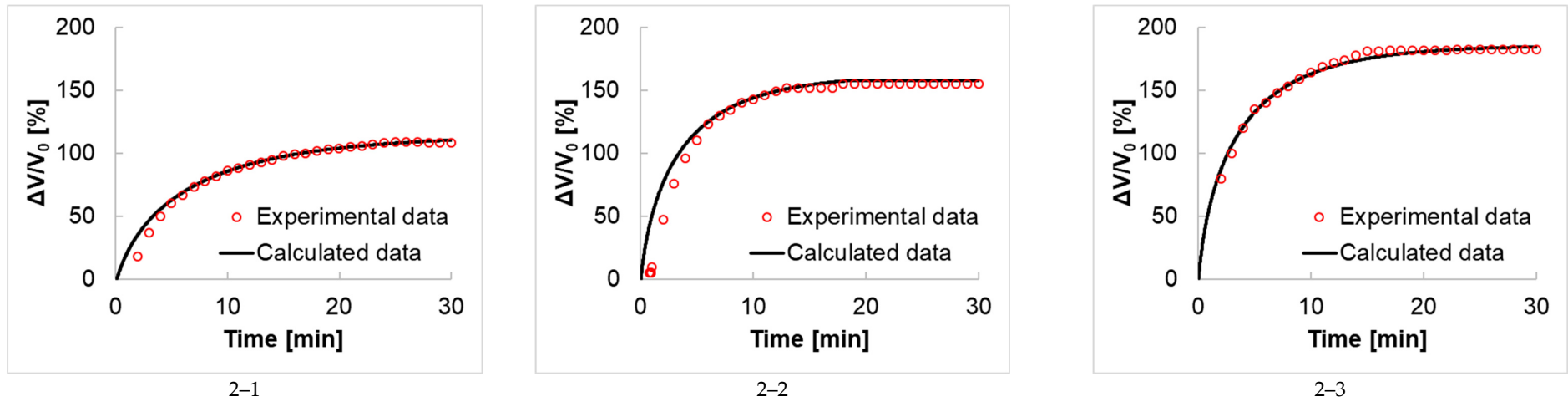


Figure 12. Experimental and calculated data of the kinetics of phase transitions at target parameters of 313 K, 7.80 MPa: experiments conducted without an alginate gel (see Table 1).

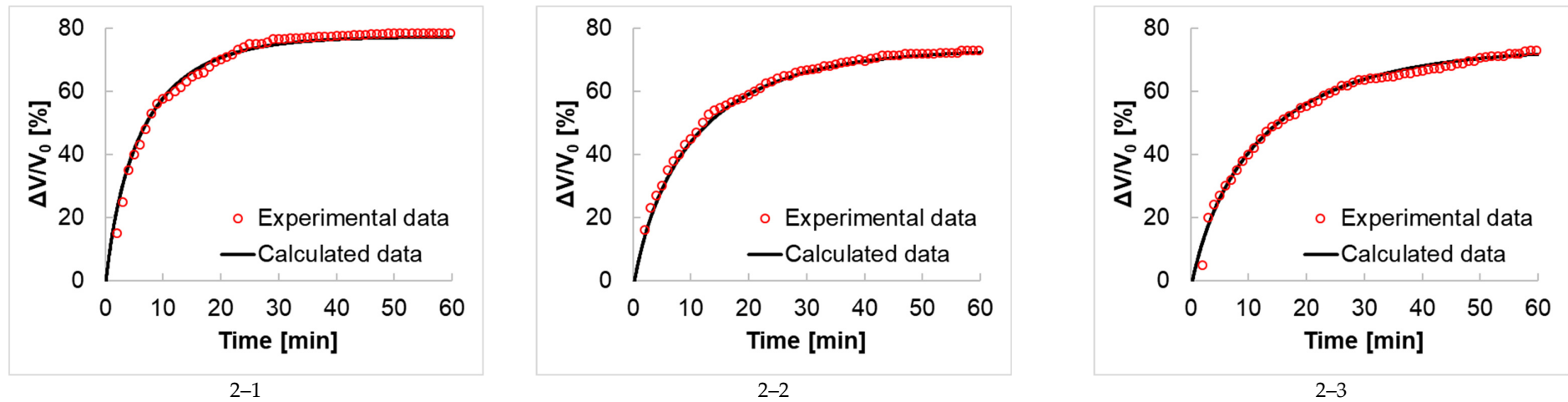


Figure 13. Experimental and calculated data of the kinetics of phase transitions at target parameters of 313 K, 7.80 MPa: experiments conducted with an alginate gel (see Table 2).

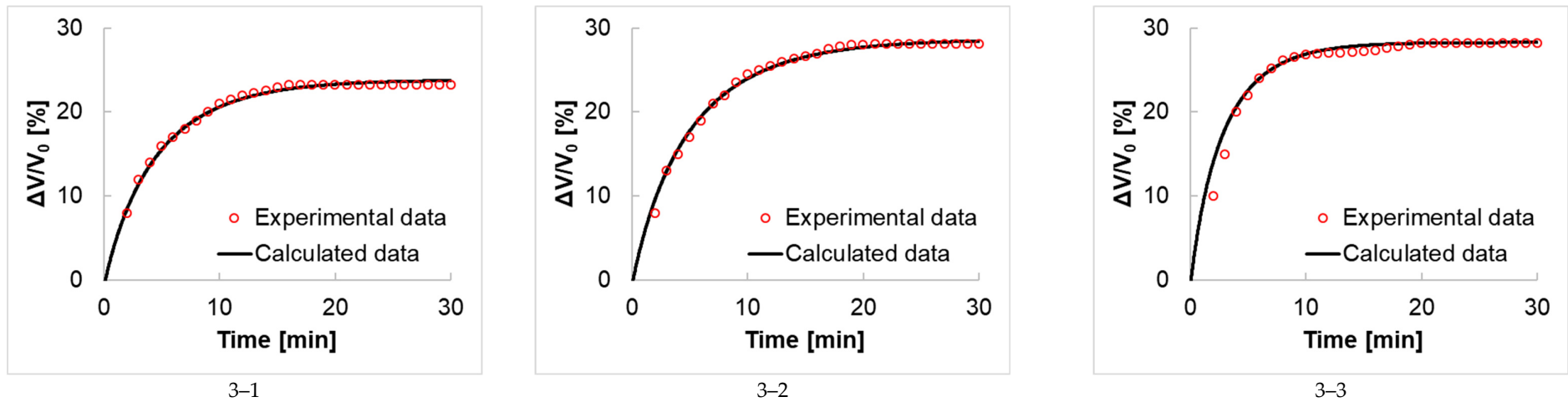


Figure 14. Experimental and calculated data of the kinetics of phase transitions at target parameters of 333 K, 6.30 MPa: experiments conducted without an alginate gel (see Table 1).

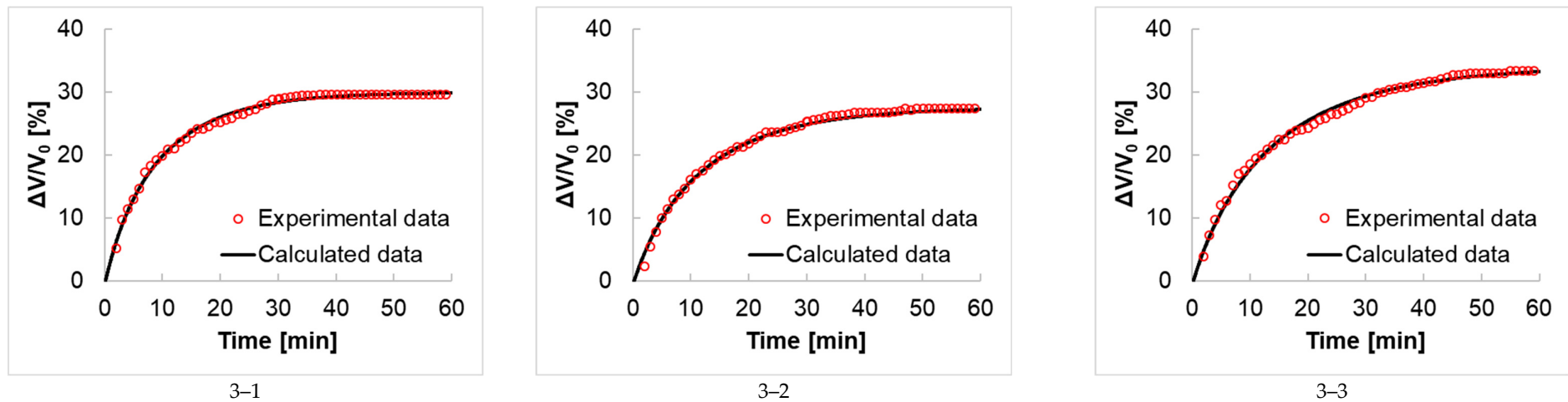


Figure 15. Experimental and calculated data of the kinetics of phase transitions at target parameters of 333 K, 6.30 MPa: experiments conducted with an alginate gel (see Table 2).

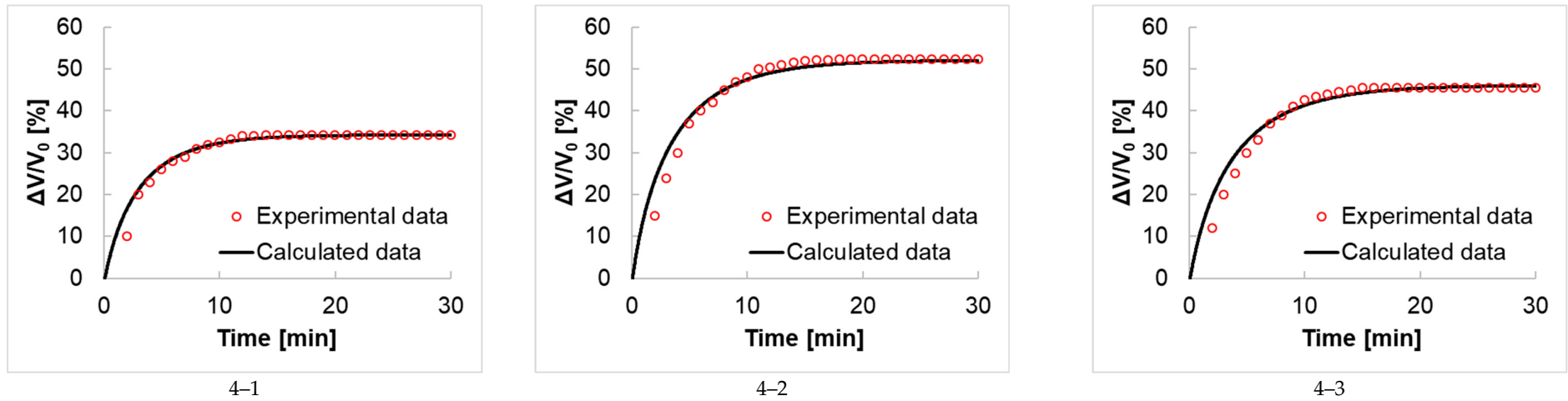


Figure 16. Experimental and calculated data of the kinetics of phase transitions at target parameters of 333 K, 7.80 MPa: experiments conducted without an alginate gel (see Table 1).

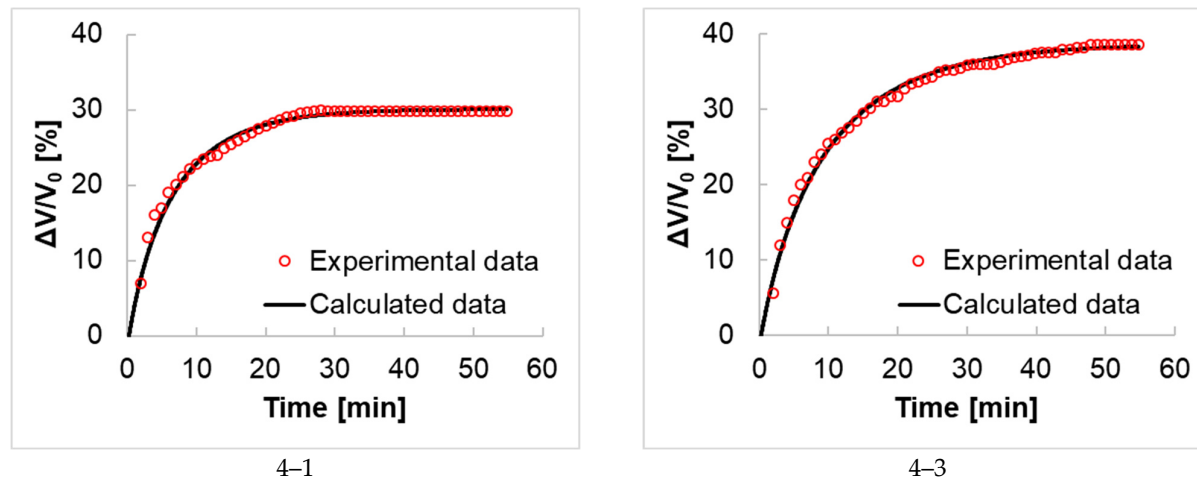


Figure 17. Experimental and calculated data of the kinetics of phase transitions at target parameters of 333 K, 7.80 MPa: experiments conducted with an alginate gel (see Table 2).

Table 3. Calculated data of the kinetics of phase transitions.

	CO ₂ Density, kg/m ³	Experiment	Average Error of the Calculated Data of Kinetic Curves (Error), %	Calculated Mass Transfer Coefficient, kg/(m ² ·s)	Average Value of the Mass Transfer Coefficient, kg/(m ² ·s)	Calculated Equilibrium Mole Fraction of CO ₂ in the Liquid Phase, mol/mol	Equilibrium Mole Fraction of CO ₂ in the Liquid Phase from [22–24,50–56], mol/mol
Without gel T = 313 K, P = 6.3 MPa	164	1–1	1.00	0.0577	0.0655	0.44	0.47
		1–2	1.92	0.0446		0.56	0.52
		1–3	1.02	0.0864		0.59	0.52
With gel T = 313 K, P = 6.3 MPa	164	1–1	1.20	0.0500	0.0396	0.59	0.51
		1–2	1.40	0.0227		0.56	0.50
		1–3	1.65	0.0460		0.62	0.52
Without gel T = 313 K, P = 7.8 MPa	267	2–1	0.92	0.1032	0.2361	0.73	0.88
		2–2	3.46	0.2814		0.79	0.95
		2–3	2.77	0.3237		0.81	0.86
With gel T = 313 K, P = 7.8 MPa	267	2–1	1.27	0.0673	0.0469	0.65	0.83
		2–2	3.23	0.0395		0.64	0.91
		2–3	1.94	0.0338		0.64	0.85
Without gel T = 333 K, P = 6.3 MPa	134	3–1	3.19	0.0390	0.0484	0.36	0.38
		3–2	3.72	0.0386		0.40	0.37
		3–3	0.79	0.0676		0.40	0.41
With gel T = 333 K, P = 6.3 MPa	134	3–1	1.47	0.0224	0.0182	0.41	0.37
		3–2	0.92	0.0164		0.39	0.37
		3–3	2.03	0.0157		0.44	0.37
Without gel T = 333 K, P = 7.8 MPa	184	4–1	1.56	0.0742	0.0773	0.45	0.48
		4–2	1.18	0.0861		0.55	0.52
		4–3	1.76	0.0716		0.52	0.48
With gel T = 333 K, P = 7.8 MPa	184	4–1	2.38	0.0318	0.0288	0.42	0.51
		4–3	2.70	0.0257		0.48	0.50

Table 3 shows that the mass transfer coefficients and the equilibrium mole fraction of CO₂ in the liquid phase can differ significantly since the binary system is sensitive to external parameters. The most obvious is the effect of the porous body on the rate of the process. A system with an alginate gel takes longer to reach equilibrium than a system without a gel. For the system at 313 K and 6.3 MPa, the mass transfer coefficient is reduced in 1.6 times; at 313 K and 7.8 MPa, in 5.0 times; at 333 K and 6.3 MPa, in 2.7 times; and at 333 K and 7.8 MPa, in 2.7 times. The mass transfer coefficient for the system without the gel decreases in 1.3 times with an isobaric increase in temperature by 20 degrees at 6.3 MPa and decreases in 3.1 times with an increase in temperature by 20 degrees at 7.8 MPa. The mass transfer coefficient for the system with the gel decreases in 2.2 times with an isobaric increase in temperature by 20 degrees at 6.3 MPa and decreases in 1.6 times with increase in temperature at 7.8 MPa. Moreover, the mass transfer coefficient increases for all cases with an isothermal pressure increase. It increases in 3.8 times for the system without the gel and in 1.2 times for the system with the gel at 313 K and increases in 1.6 times for both systems with and without the gel at 333 K. It can be noted that the effect of pressure is less significant in a system with the presence of a gel.

The specified behavior of the system can be directly related to the density of carbon dioxide. When changing external parameters, its density changes significantly. To demonstrate the influence of the density of carbon dioxide on the mass transfer coefficient, the data were plotted in Figure 18. The target external parameters are also marked in the picture. This applies for data without the gel and for data with the gel. It is important to note that the influence of the density of carbon dioxide is more interesting than the influence of the density of 2-propanol, as the density of 2-propanol changes insignificantly within the considered parameters.

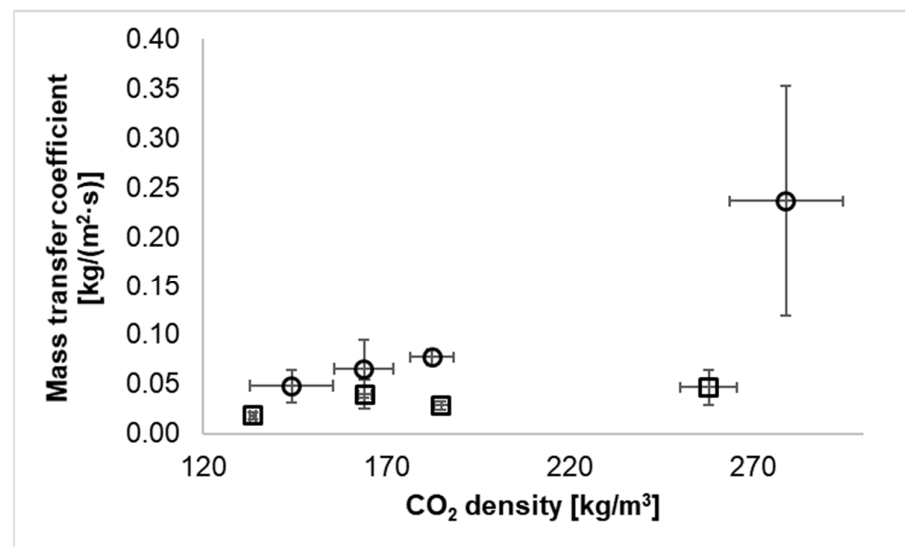


Figure 18. Mass transfer coefficient at different densities of CO₂. (o—without gel, □—with gel).

The data clearly show that with an increase in the density, an increase in the coefficient of mass transfer occurs, that is, the rate of the process increases. This is due to the increased diffusion rate at higher densities of CO₂. This is mainly true for systems without a gel. Moreover, it can be seen that the behavior of the system differs significantly at different pressures. As noted earlier, more obvious differences in the rate of the process in the system without the gel and in the system with the gel are noticeable at 7.8 MPa than at 6.3 MPa. The critical pressure of the mixture “2-propanol—CO₂” at temperature 313 K is 8.29 MPa, and at temperature 333 K it is 10.35 MPa [23]. Thus, for both temperatures, the system at 7.8 MPa is closer to the critical parameters than the system at 6.3 MPa. It is obvious that under conditions near the critical parameters, a convective transport can arise. This is due to the fact that the densities of the gas and liquid phases become closer to each other, and

their mutual mixing is facilitated. The presence of a porous body (alginate gel) significantly reduces the effect of convective transport. Thus, the rate of the mass transfer does not increase as noticeably with an increase in the density of CO₂ and with the approach of the critical parameters for the system with alginate gel.

It can be seen that the closer the system parameters are to the critical parameters, the more difficult it becomes to maintain constant process parameters. Thus, there is a significant increase in the confidence intervals at the parameters of 313 K and 7.8 MPa.

The calculated equilibrium mole fractions of CO₂ in the liquid phase are close to the literature data (Table 3). The average error of the calculated equilibrium mole fractions for all experiments is 13%. Moreover, the highest error is observed for experiments at the external target parameters 313 K and 7.8 MPa (25%), which are close to the critical parameters of the “2-propanol—CO₂” system. This is due to the fact that the system in near critical conditions is less stable, and PR-EoS is worse for describing the system in a subcritical state.

4. Conclusions

Experimental studies of the kinetics of “2-propanol—CO₂” system phase transitions under high pressure have been carried out. It was found that with an isobaric increase in temperature, the solubility of CO₂ in 2-propanol decreases, and with an isothermal pressure increase, on the contrary, it increases. The system with alginate gel takes more than two times longer to reach a state of equilibrium. As a result of the experimental study, the kinetic curves of phase transitions were obtained using a new method with and without the presence of a porous body (alginate gel).

A new approach was proposed for calculating the mass transfer coefficient in the system under consideration. It was calculated using the Peng-Robinson equation of state with Van der Waals mixing rules. The proposed equations accurately describe the mass transfer process, and the error between the calculated and experimental data was, on average, 2%. The calculated values of the mass transfer coefficient and the analysis led to an important conclusion about the influence of external parameters on the transport rate in the heterogeneous system “2-propanol—CO₂” with and without the presence of a porous body (alginate gel).

The data can be used to study the kinetic characteristics of many supercritical processes. The proposed approach can be used for optimization of processes that are carried out under conditions close to critical. This will help in the production of aerogels, and in some cases, it can be used in supercritical extraction, drying, etc.

Author Contributions: Conceptualization, A.L. and E.S.; methodology, A.L. and E.S.; software, A.L. and E.S.; validation, A.L., M.M. and E.S.; formal analysis, E.S.; investigation, E.S.; resources, M.M.; data curation, E.S.; writing—original draft preparation, A.L. and E.S.; writing—review and editing, E.S.; visualization, E.S.; supervision, A.L. and M.M.; project administration, E.S. and A.L.; funding acquisition, A.L. All authors have read and agreed to the published version of the manuscript.

Funding: Research was funded by the grant from Russian Science Foundation (Project No. 22-79-00154).

Data Availability Statement: The experimental data and code will be provided upon request.

Conflicts of Interest: The authors declare no conflict of interest.

Appendix A Supplementary Data (Liquid Phase Height and Measurement Error)

This section describes the determination of the height of the liquid phase h in the photographic image and its measurement errors. For a more accurate determination of the height, a grid of five parallel vertical lines (red lines in Figure A1) perpendicular to the diameter of the apparatus was constructed. An example of the grid is shown in Figure A1.

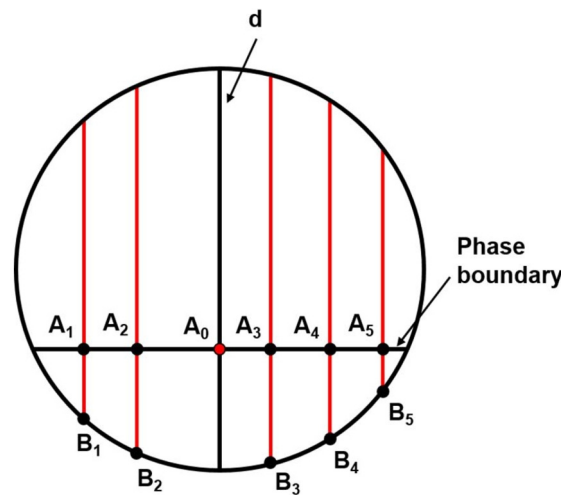


Figure A1. Auxiliary grid for determining the height of the liquid phase h .

This grid was superimposed on the photographic images of the system in the apparatus in such a way that the phase boundary coincided with the surface shown in Figure A1. To determine the height h , the values of perpendiculars of each line that intersect with the circle that represents the wall of the apparatus (A_iB_i) and the distances from the center of the interface A_0 to the vertical line A_i (A_0A_i) are used. With the help of the obtained data, the height of the liquid phase h was recalculated according to the equation

$$h_i = \frac{d}{2} - \sqrt{\left(\frac{d}{2}\right)^2 - A_0A_i^2} + A_iB_i \tag{A1}$$

Table A1 presents the data obtained from a single photographic image at the time $\tau = 20$ min for the “2-propanol—CO₂” system (experiment 4–2, Table 1).

Table A1. Auxiliary segment data used to determine the height of the liquid phase.

Vertical Line №, i	A_0A_i	A_iB_i	h_i
1	4.15	3.31	4.66
2	2.28	4.23	4.61
3	1.59	4.37	4.55
4	3.49	3.60	4.52
5	5.19	2.12	4.40

Next, the real height of the liquid phase H was calculated according to Equation (1) and its average value \bar{H} at five points ($n = 5$). Then, the mean absolute deviation of the height values was determined using equation

$$\sigma = \frac{\sum_{i=1}^n |H_i - \bar{H}|}{n} \tag{A2}$$

After determining the height and the calculation error, a curve of the change of the height of the liquid phase with a vertical average deviation was constructed for each photographic image. An example of constructing the experiment curve 4–2 (Table 1) is shown in Figure A2.

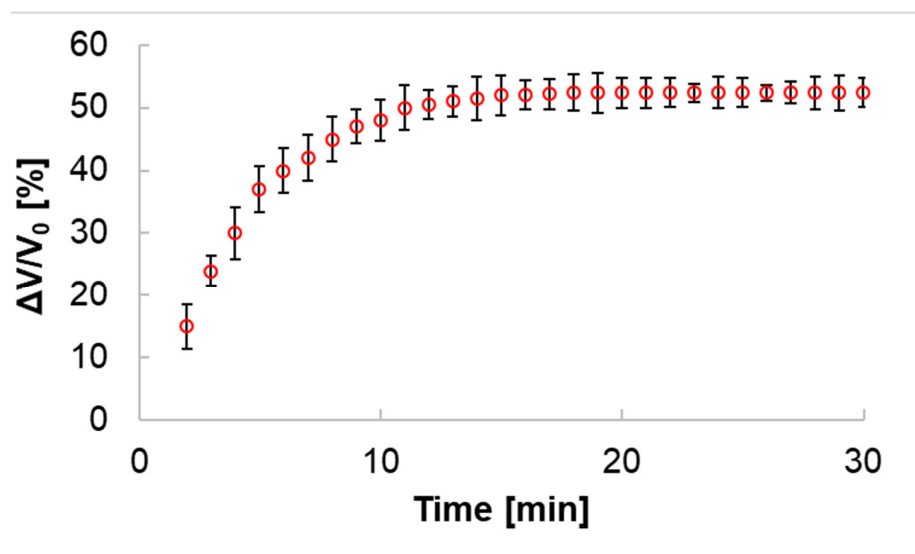


Figure A2. Kinetics of the change of the “2-propanol—CO₂” system liquid phase height (experiment 4—2, Table 1).

When studying further the change of the liquid phase volume, the vertical average deviation is not indicated in the curves (Figures 5 and 6), since they are within the limits shown in Figure A2, and the average deviation of the height of the liquid phase does not exceed 5%. The height of the liquid phase obtained in this way is used to further determine the liquid phase volume at each time using Equation (2).

References

- Hegel, P.; Martín, L.; Popovich, C.; Damiani, C.; Pancaldi, S.; Pereda, S.; Leonardi, P. Biodiesel Production from Neochloris Oleoabundans by Supercritical Technology. *Chem. Eng. Process. Process Intensif.* **2017**, *121*, 232–239. [[CrossRef](#)]
- Gracia, E.; García, M.T.; Rodríguez, J.F.; de Lucas, A.; Gracia, I. Improvement of PLGA Loading and Release of Curcumin by Supercritical Technology. *J. Supercrit. Fluids* **2018**, *141*, 60–67. [[CrossRef](#)]
- Arango-Ruiz, Á.; Martín, Á.; Cosero, M.J.; Jiménez, C.; Londoño, J. Encapsulation of Curcumin Using Supercritical Antisolvent (SAS) Technology to Improve Its Stability and Solubility in Water. *Food Chem.* **2018**, *258*, 156–163. [[CrossRef](#)] [[PubMed](#)]
- Johner, J.C.F.; Hatami, T.; Meireles, M.A.A. Developing a Supercritical Fluid Extraction Method Assisted by Cold Pressing for Extraction of Pequi (*Caryocar Brasiliense*). *J. Supercrit. Fluids* **2018**, *137*, 34–39. [[CrossRef](#)]
- Kohli, R. Applications of Supercritical Carbon Dioxide for Removal of Surface Contaminants. In *Developments in Surface Contamination and Cleaning: Applications of Cleaning Techniques*; Elsevier: Amsterdam, The Netherlands, 2018; Volume 11, pp. 209–249, ISBN 9780128155776.
- Nikolai, P.; Rabiyat, B.; Aliev, A.; Abdulgatov, I. Supercritical CO₂: Properties and Technological Applications—A Review. *J. Therm. Sci.* **2019**, *28*, 394–430. [[CrossRef](#)]
- De Souza, A.T.; Benazzi, T.L.; Grings, M.B.; Cabral, V.; Antônio da Silva, E.; Cardozo-Filho, L.; Ceva Antunes, O.A. Supercritical Extraction Process and Phase Equilibrium of Candeia (*Eremanthus Erythropappus*) Oil Using Supercritical Carbon Dioxide. *J. Supercrit. Fluids* **2008**, *47*, 182–187. [[CrossRef](#)]
- Scopel, R.; Falcão, M.A.; Lucas, A.M.; Almeida, R.N.; Gandolfi, P.H.K.; Cassel, E.; Vargas, R.M.F. Supercritical Fluid Extraction from *Syzygium aromaticum* Buds: Phase Equilibrium, Mathematical Modeling and Antimicrobial Activity. *J. Supercrit. Fluids* **2014**, *92*, 223–230. [[CrossRef](#)]
- Sierra-Pallares, J.; del Valle, J.G.; Bueno, C.M.; García, J.; Castro, F. High-Pressure Fluid Flow in Carbon Dioxide—Organic Solvent Mixing Layers. Equilibrium Models and the Prediction of Phase Transitions. *J. Supercrit. Fluids* **2020**, *169*, 105024. [[CrossRef](#)]
- De Marco, I.; Knauer, O.; Cice, F.; Braeuer, A.; Reverchon, E. Interactions of Phase Equilibria, Jet Fluid Dynamics and Mass Transfer during Supercritical Antisolvent Micronization: The Influence of Solvents. *Chem. Eng. J.* **2012**, *203*, 71–80. [[CrossRef](#)]
- Smirnova, I.; Gurikov, P. Aerogel Production: Current Status, Research Directions, and Future Opportunities. *J. Supercrit. Fluids* **2018**, *134*, 228–233. [[CrossRef](#)]
- Lazrag, M.; Lemaitre, C.; Castel, C.; Hannachi, A.; Barth, D. Aerogel Production by Supercritical Drying of Organogels: Experimental Study and Modelling Investigation of Drying Kinetics. *J. Supercrit. Fluids* **2018**, *140*, 394–405. [[CrossRef](#)]
- Chen, D.; Gao, H.; Liu, P.; Huang, P.; Huang, X. Directly Ambient Pressure Dried Robust Bridged Silsesquioxane and Methylsiloxane Aerogels: Effects of Precursors and Solvents. *RSC Adv.* **2019**, *9*, 8664–8671. [[CrossRef](#)] [[PubMed](#)]

14. Rao, A.P.; Rao, A.V.; Gurav, J.L. Effect of Protic Solvents on the Physical Properties of the Ambient Pressure Dried Hydrophobic Silica Aerogels Using Sodium Silicate Precursor. *J. Porous Mater.* **2008**, *15*, 507–512. [[CrossRef](#)]
15. Tripathi, A.; Parsons, G.N.; Khan, S.A.; Rojas, O.J. Synthesis of Organic Aerogels with Tailorable Morphology and Strength by Controlled Solvent Swelling Following Hansen Solubility. *Sci. Rep.* **2018**, *8*, 2106. [[CrossRef](#)]
16. Omranpour, H.; Motahari, S. Effects of Processing Conditions on Silica Aerogel during Aging: Role of Solvent, Time and Temperature. *J. Non-Cryst. Solids* **2013**, *379*, 7–11. [[CrossRef](#)]
17. Bueno, A.; Selmer, I.; SP, R.; Gurikov, P.; Lölsberg, W.; Weinrich, D.; Fricke, M.; Smirnova, I. First Evidence of Solvent Spillage under Subcritical Conditions in Aerogel Production. *Ind. Eng. Chem. Res.* **2018**, *57*, 8698–8707. [[CrossRef](#)]
18. Gui, X.; Tang, Z.; Fei, W. Solubility of CO₂ in Alcohols, Glycols, Ethers, and Ketones at High Pressures from (288.15 to 318.15) K. *J. Chem. Eng. Data* **2011**, *56*, 2420–2429. [[CrossRef](#)]
19. Décultot, M.; Ledoux, A.; Fournier-Salaün, M.C.; Estel, L. Solubility of CO₂ in Methanol, Ethanol, 1,2-Propanediol and Glycerol from 283.15 K to 373.15 K and up to 6.0 MPa. *J. Chem. Thermodyn.* **2019**, *138*, 67–77. [[CrossRef](#)]
20. Liu, H.; Gao, H.; Idem, R.; Tontiwachwuthikul, P.; Liang, Z. Analysis of CO₂ Solubility and Absorption Heat into 1-Dimethylamino-2-Propanol Solution. *Chem. Eng. Sci.* **2017**, *170*, 3–15. [[CrossRef](#)]
21. Lazzaroni, M.J.; Bush, D.; Brown, J.S.; Eckert, C.A. High-Pressure Vapor–Liquid Equilibria of Some Carbon Dioxide + Organic Binary Systems. *J. Chem. Eng. Data* **2005**, *50*, 60–65. [[CrossRef](#)]
22. Bamberger, A.; Maurer, G. High-Pressure (Vapour + Liquid) Equilibria in (Carbon Dioxide + Acetone or 2-Propanol) at Temperatures from 293 K to 333 K. *J. Chem. Thermodyn.* **2000**, *32*, 685–700. [[CrossRef](#)]
23. Radosz, M. Vapor-Liquid Equilibrium for 2-Propanol and Carbon Dioxide. *J. Chem. Eng. Data* **1986**, *31*, 43–45. [[CrossRef](#)]
24. Ziegler, J.W.; Chester, T.L.; Innis, D.P.; Page, S.H.; Dorsey, J.G. Supercritical Fluid Flow Injection Method for Mapping Liquid–Vapor Critical Loci of Binary Mixtures Containing CO₂. In *Innovations in Supercritical Fluids*; ACS Symposium Series; American Chemical Society: Washington, DC, USA, 1995; Volume 608, pp. 93–110, ISBN 978-0-8412-3324-9.
25. Elizalde-Solis, O.; Galicia-Luna, L.A.; Camacho-Camacho, L.E. High-Pressure Vapor–Liquid Equilibria for CO₂+alkanol Systems and Densities of n-Dodecane and n-Tridecane. *Fluid Phase Equilibria* **2007**, *259*, 23–32. [[CrossRef](#)]
26. Tachiwaki, T. Supercritical Fluid Drying of Aqueous 2-Propanol Suspension. *Dry. Technol.* **2004**, *22*, 325–334. [[CrossRef](#)]
27. Egerer, K.; Brandl, F.; Golzari, N.; Beuermann, S. Recycling of Printed Circuit Boards Employing Supercritical Carbon Dioxide. *Mater. Sci. Forum* **2019**, *959*, 100–106. [[CrossRef](#)]
28. Fateen, S.E.K.; Khalil, M.M.; Elnabawy, A.O. Semi-Empirical Correlation for Binary Interaction Parameters of the Peng-Robinson Equation of State with the van Der Waals Mixing Rules for the Prediction of High-Pressure Vapor-Liquid Equilibrium. *J. Adv. Res.* **2013**, *4*, 137–145. [[CrossRef](#)] [[PubMed](#)]
29. Muhr, A.H.; Blanshard, J.M.V. Diffusion in Gels. *Polymer* **1982**, *23*, 1012–1026. [[CrossRef](#)]
30. Masmoudi, Y.; Rigacci, A.; Ilbizian, P.; Cauneau, F.; Achard, P. Diffusion During the Supercritical Drying of Silica Gels. *Dry. Technol.* **2006**, *24*, 1121–1125. [[CrossRef](#)]
31. Lebedev, A.; Suslova, E.; Troyankin, A.; Lovskaya, D. Investigation of Aerogel Production Processes: Solvent Exchange under High Pressure Combined with Supercritical Drying in One Apparatus. *Gels* **2021**, *7*, 4. [[CrossRef](#)]
32. Peng, D.-Y.; Robinson, D.B. A New Two-Constant Equation of State. *Ind. Eng. Chem. Fundam.* **1976**, *15*, 59–64. [[CrossRef](#)]
33. Markočič, E.; Knez, Ž. Redlich-Kwong Equation of State for Modelling the Solubility of Methane in Water over a Wide Range of Pressures and Temperatures. *Fluid Phase Equilibria* **2016**, *408*, 108–114. [[CrossRef](#)]
34. Su, C.S. Prediction of Volumetric Properties of Carbon Dioxide-Expanded Organic Solvents Using the Predictive Soave-Redlich-Kwong (PSRK) Equation of State. *J. Supercrit. Fluids* **2012**, *72*, 223–231. [[CrossRef](#)]
35. Gregorowicz, J.; De Loos, T.W. Modelling of the Three Phase LLV Region for Ternary Hydrocarbon Mixtures with the Soave-Redlich-Kwong Equation of State. *Fluid Phase Equilibria* **1996**, *118*, 121–132. [[CrossRef](#)]
36. Forero, G.L.A.; Velásquez, J.J. The Patel-Teja and the Peng-Robinson EoSs Performance When Soave Alpha Function Is Replaced by an Exponential Function. *Fluid Phase Equilibria* **2012**, *332*, 55–76. [[CrossRef](#)]
37. Valderrama, J.O.; Cardona, L.F.; Rojas, R.E. Correlation of Ionic Liquid Viscosity Using Valderrama-Patel-Teja Cubic Equation of State and the Geometric Similitude Concept. Part II: Binary Mixtures of Ionic Liquids. *Fluid Phase Equilibria* **2019**, *497*, 178–194. [[CrossRef](#)]
38. Barragán-Aroche, J.F.; Bazúa-Rueda, E.R. A Local Composition Extension of the van Der Waals Mixing Rule for PR Cubic Equation of State. *Fluid Phase Equilibria* **2005**, *227*, 97–112. [[CrossRef](#)]
39. Grgurić, I.R.; Šerbanović, S.P.; Kijevčanin, M.L.; Tasić, A.Ž.; Djordjević, B.D. Volumetric Properties of the Ternary System Ethanol + 2-Butanone + Benzene by the van Der Waals and Twu-Coon-Bluck-Tilton Mixing Rules: Experimental Data, Correlation and Prediction. *Thermochim. Acta* **2004**, *412*, 25–31. [[CrossRef](#)]
40. Forero, G.; Luis, A.; Velasquez, J.; Jorge, A. Modeling the Liquid-Liquid Equilibria of Polar Aprotic Solvents/Alkanes Type Mixtures Using a Modified PR EoS and the Huron-Vidal Mixing Rules. *J. Mol. Liq.* **2019**, *292*, 111380. [[CrossRef](#)]
41. Velásquez, J.; Jorge, A.; Forero, G.; Luis, A. Calculation of Complex Phase Equilibria of DMF/Alkane and Acetonitrile/Alkane Systems Using a Modified Peng-Robinson EoS and the Huron-Vidal Mixing Rules. *J. Mol. Liq.* **2017**, *243*, 600–610. [[CrossRef](#)]
42. López, J.A.; Cardona, C.A. Phase Equilibrium Calculations for Carbon Dioxide + N-Alkanes Binary Mixtures with the Wong-Sandler Mixing Rules. *Fluid Phase Equilibria* **2006**, *239*, 206–212. [[CrossRef](#)]

43. Espanani, R.; Miller, A.; Jacoby, W. Prediction of Vapor-Liquid Equilibria for Mixtures of Low Boiling Point Compounds Using Wong-Sandler Mixing Rule and EOS/GE Model. *Chem. Eng. Sci.* **2016**, *152*, 343–350. [[CrossRef](#)]
44. Menshutina, N.V.; Lovskaya, D.D.; Lebedev, A.E.; Lebedev, E.A. Production of Sodium Alginate-Based Aerogel Particles Using Supercritical Drying in Units with Different Volumes. *Russ. J. Phys. Chem. B* **2017**, *11*, 1296–1305. [[CrossRef](#)]
45. Bolten, D.; Johannsen, M. Influence of 2-Propanol on Adsorption Equilibria of α - and δ -Tocopherol from Supercritical Carbon Dioxide on Silica Gel. *J. Chem. Eng. Data* **2006**, *51*, 2132–2137. [[CrossRef](#)]
46. Lovskaya, D.; Menshutina, N. Alginate-Based Aerogel Particles as Drug Delivery Systems: Investigation of the Supercritical Adsorption and In Vitro Evaluations. *Materials* **2020**, *13*, 329. [[CrossRef](#)] [[PubMed](#)]
47. Gaudio, P.D.; Auriemma, G.; Mencherini, T.; Porta, G.D.; Reverchon, E.; Aquino, R.P. Design of Alginate-Based Aerogel for Nonsteroidal Anti-Inflammatory Drugs Controlled Delivery Systems Using Prilling and Supercritical-Assisted Drying. *J. Pharm. Sci.* **2013**, *102*, 185–194. [[CrossRef](#)]
48. Lebedev, A.E.; Katalevich, A.M.; Menshutina, N.V. Modeling and Scale-up of Supercritical Fluid Processes. Part I: Supercritical Drying. *J. Supercrit. Fluids* **2015**, *106*, 122–132. [[CrossRef](#)]
49. Lipschutz, S.; Liu, J.; Spiegel, T. *Schaum's Outline: Mathematical Handbook of Formulas and Tables*, 4th ed.; McGraw-Hill Education: Sydney, Australia, 2018; ISBN 978-1-260-01053-4.
50. Zevnik, L.; Levec, J. Hydrogen Solubility in CO₂-Expanded 2-Propanol and in Propane-Expanded 2-Propanol Determined by an Acoustic Sensor. *J. Supercrit. Fluids* **2007**, *41*, 335–342. [[CrossRef](#)]
51. Lim, J.S.; Jung, Y.G.; Yoo, K.-P. High-Pressure Vapor–Liquid Equilibria for the Binary Mixtures of Carbon Dioxide + Isopropanol (IPA). *J. Chem. Eng. Data* **2007**, *52*, 2405–2408. [[CrossRef](#)]
52. Secuianu, C.; Feroiu, V.; Geană, D. High-Pressure Vapor-Liquid Equilibria in the System Carbon Dioxide and 2-Propanol at Temperatures from 293.25 K to 323.15 K. *J. Chem. Eng. Data* **2003**, *48*, 1384–1386. [[CrossRef](#)]
53. Khalil, W.; Coquelet, C.; Richon, D. High-Pressure Vapor–Liquid Equilibria, Liquid Densities, and Excess Molar Volumes for the Carbon Dioxide + 2-Propanol System from (308.10 to 348.00) K. *J. Chem. Eng. Data* **2007**, *52*, 2032–2040. [[CrossRef](#)]
54. Sima, S.; Racovita, R.; Dinca, C.; Feroiu, V.; Secuianu, C. Phase Equilibria Calculations for Carbon Dioxide + 2-Propanol System. *UPB Sci. Bull. Ser. B Chem. Mater. Sci.* **2017**, *79*, 11–24.
55. Yaginuma, R.; Nakajima, T.; Tanaka, H.; Kato, M. Densities of Carbon Dioxide + 2-Propanol at 313.15 K and Pressures to 9.8 MPa. Available online: <https://pubs.acs.org/doi/pdf/10.1021/je9700028> (accessed on 2 June 2021).
56. Hsieh, C.-M.; Windmann, T.; Vrabec, J. Vapor-Liquid Equilibria of CO₂ + C1-C5 Alcohols from the Experiment and the COSMO-SAC Model. *J. Chem. Eng. Data* **2013**, *58*, 3420–3429. [[CrossRef](#)]

Disclaimer/Publisher's Note: The statements, opinions and data contained in all publications are solely those of the individual author(s) and contributor(s) and not of MDPI and/or the editor(s). MDPI and/or the editor(s) disclaim responsibility for any injury to people or property resulting from any ideas, methods, instructions or products referred to in the content.